Extended data

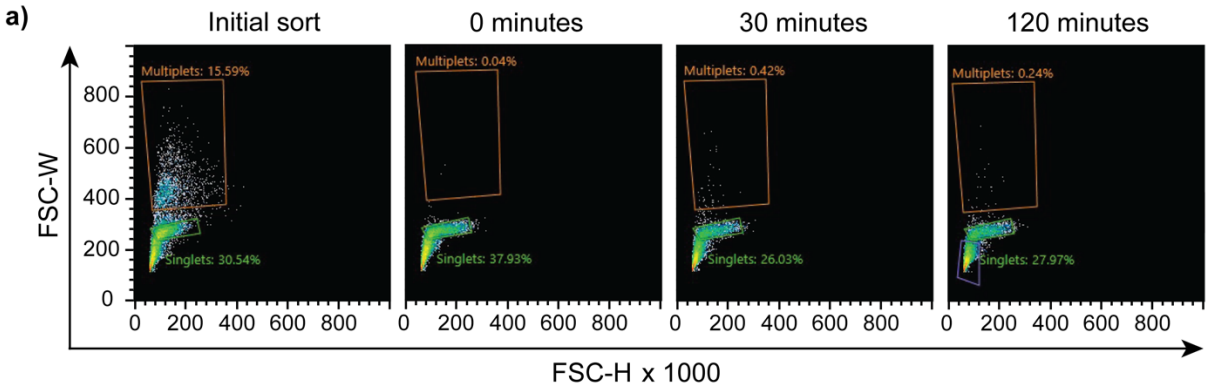

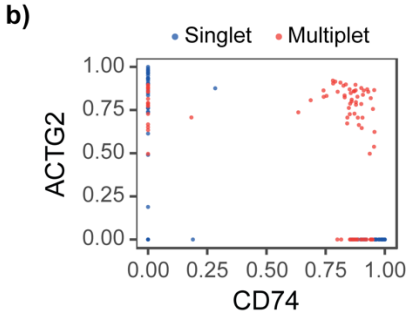

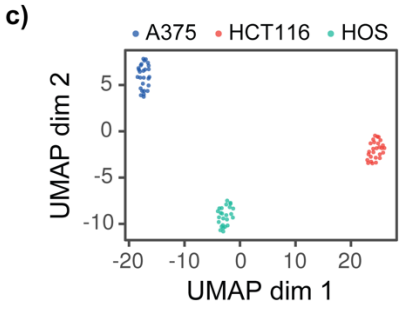

d)

Cell type	Expected	Detected
A375	65	63
HCT116	54	50
HOS	65	61

e)

Cells in multiplet	n	TPR	TNR	MCR
A375, A375, HCT116, HCT116	8	1.00	1	0.00
A375, A375, HCT116, HOS	8	0.88	NA	0.12
A375, HCT116	10	0.90	1	0.07
A375, HCT116, HOS	10	0.97	NA	0.03
A375, HOS	11	0.91	1	0.06
A375, HOS, HOS	9	1.00	1	0.00
A375, HOS, HOS, HOS	9	1.00	1	0.00
HCT116, HCT116, HOS	8	0.88	1	0.08
HCT116, HOS	10	1.00	1	0.00

Extended Data Figure 1. a) Flow cytometry analysis of re-association rate. HCT116 singlets and multiplets were sorted separately and singlets were re-analyzed after 0, 30, and 120 minutes. **b)** Analysis of A375 (CD74) and HOS (ACTG2) specific marker expression in singlets and multiplets shows co-expression is only observed in multiplets. **c)** Dimensionality reduction (UMAP) and unsupervised classification of the sorted cell line singlets. **d)** Numbers of expected (sorted) and detected (deconvoluted) cell types in cell line-based multiplets of a known composition. **e)** Cell line-based multiplets of a known composition results showing the number of samples (n), true positive rate (TPR), true negative rate (TNR), and misclassification rate (MCR) for each multiplet composition.

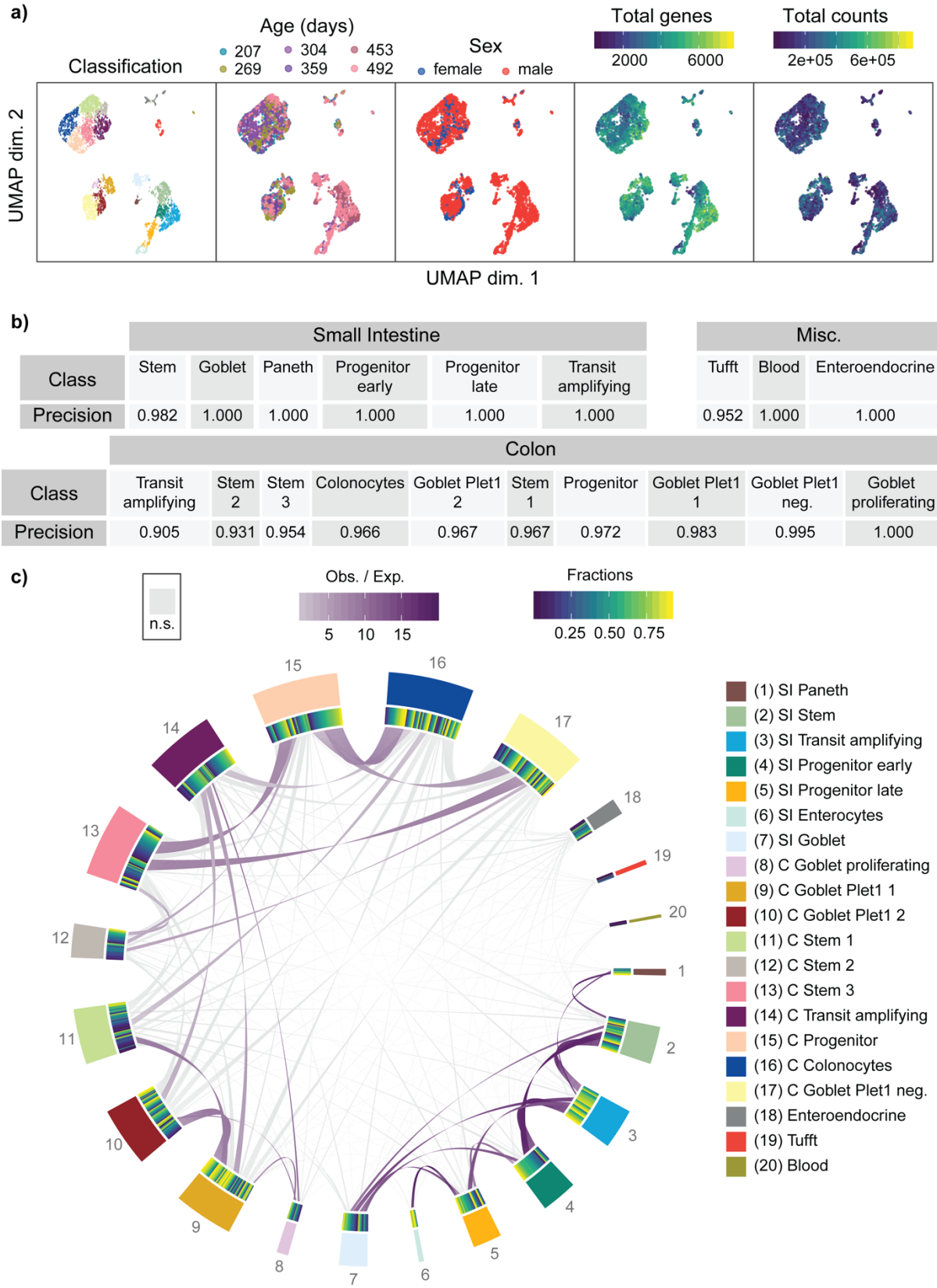

Extended Data Figure 2. a) Covariate analysis in mouse gut dataset showing a lack of correlation between covariates and classification. **b)** Deconvolution of mouse gut singlets shows a high precision for all classes indicating the validity of the classification and sufficiency of the provided features to allow discrimination between the different cell types. **c)** Deconvolution of the entire mouse gut dataset indicates a lack of enriched cross-tissue connections and thus implies a low false positive connection rate. Note that due to tissue-specific interactions, some previously non-significant connections (eg. goblet cells in small intestine) are now called as significant.

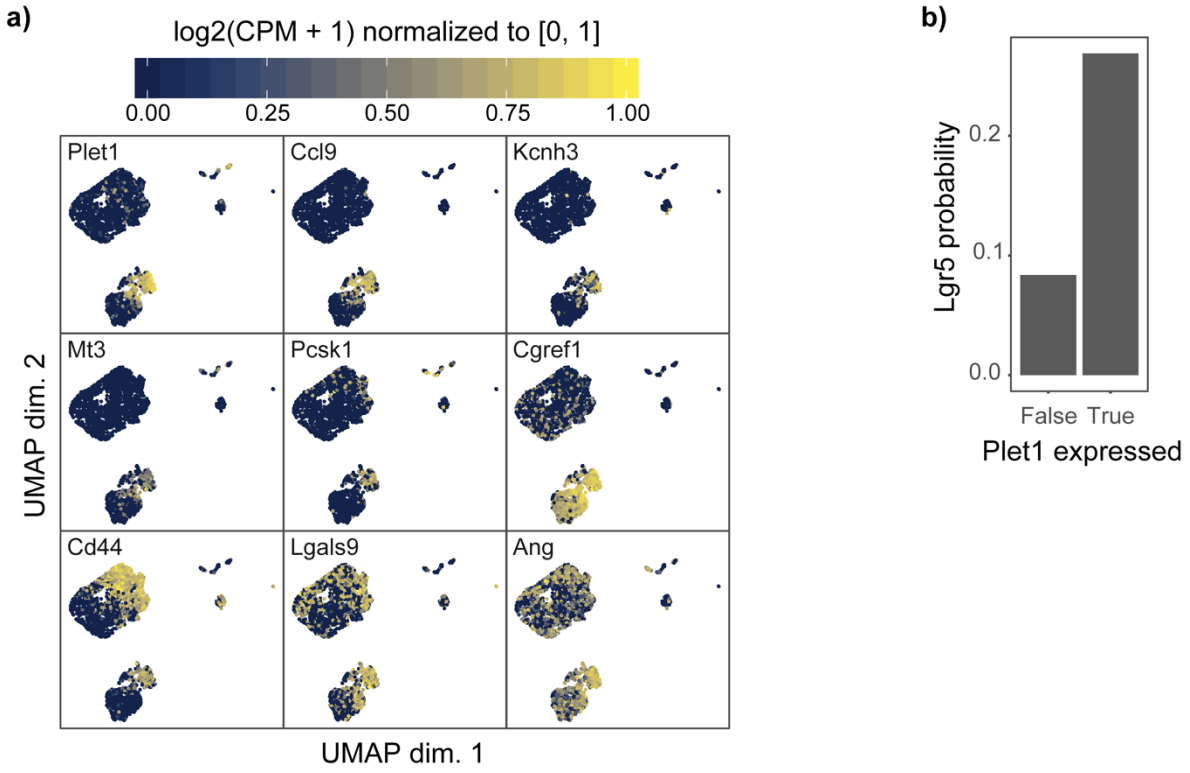

Extended Data Figure 3. a) *Plet1* differential expression genes, log2(TPM + 1) normalized to [0, 1], overlaid on the colonic epithelium UMAP. **b)** The probability of observing *Lgr5* expression in Muc2+ goblet cells dependent on *Plet1* expression.

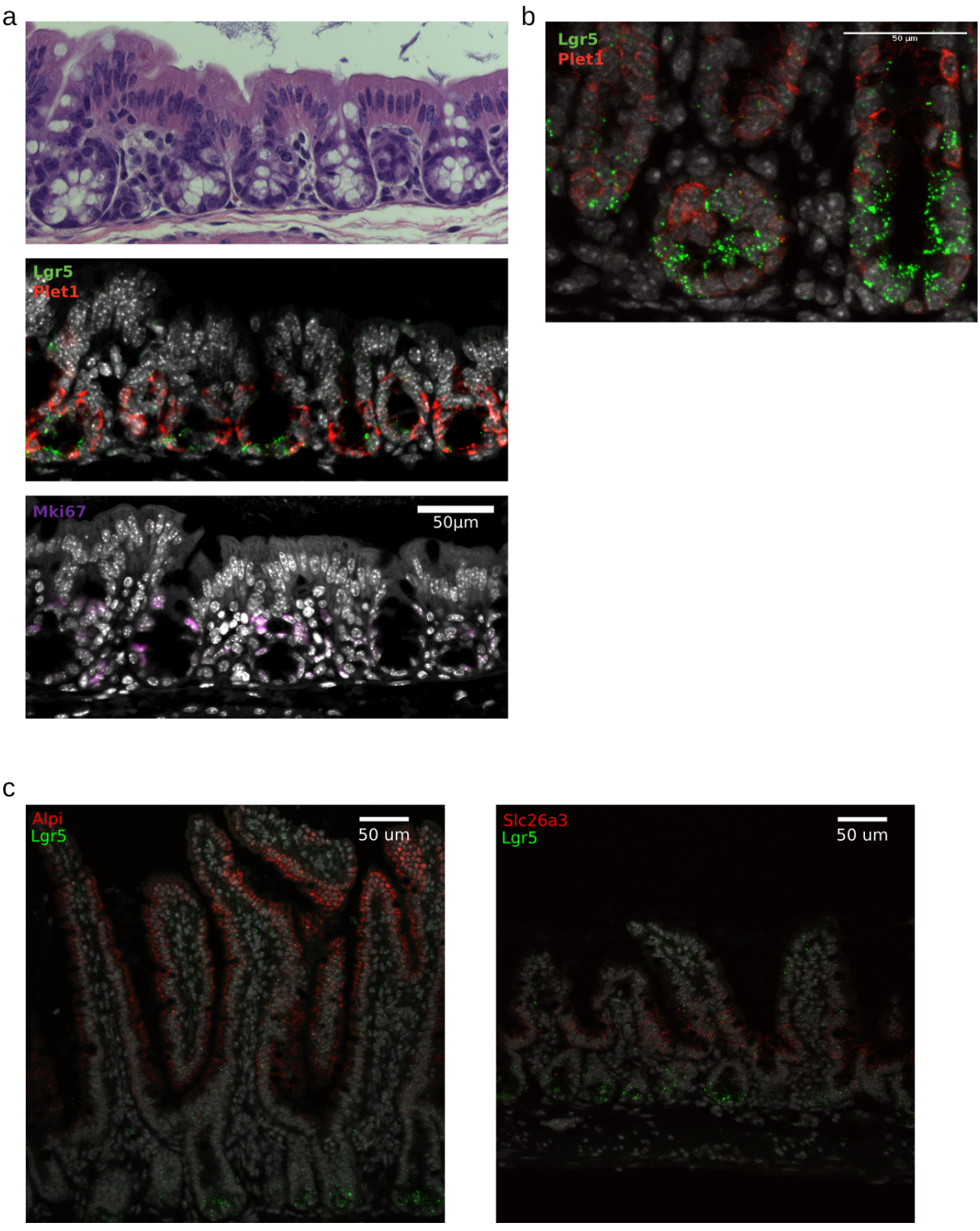

Extended Data Fig. 4. a) Consecutive slices from histologically unaffected regions of colon from a mouse treated with DSS. H&E (top), RNA ISH of *Lgr5*, *Plet1* (middle), and immunohistochemistry of Mki67 (bottom). **b)** mRNA abundance of *Lgr5* and *Plet1* at the bottom of crypts in regenerating colonic epithelium shows a similar pattern to that seen in normal healthy colon crypts. **c)** RNA ISH of stem cell distant cell types. Left: *Alpi* and *Lgr5* RNA ISH in small intestine. Large Alpi+ structures are villi. Right: *Slc26a3* and *Lgr5* RNA ISH in colon.